applied sciences

MDPI

Article

Highly Sensitive and Selective H_2S Chemical Sensor Based on ZnO Nanomaterial

Vardan Galstyan *, Nicola Poli and Elisabetta Comini

Sensor Lab, Department of Information Engineering, University of Brescia, Via Valotti 9, 25133 Brescia, Italy; nicola.poli@unibs.it (N.P.); elisabetta.comini@unibs.it (E.C.)

* Correspondence: vardan.galstyan@unibs.it

Received: 22 February 2019; Accepted: 15 March 2019; Published: 19 March 2019

Abstract: ZnO is worth evaluating for chemical sensing due to its outstanding physical and chemical properties. We report the fabrication and study of the gas sensing properties of ZnO nanomaterial for the detection of hydrogen sulfide (H_2S). This prepared material exhibited a 7400 gas sensing response when exposed to 30 ppm of H_2S in air. In addition, the structure showed a high selectivity towards H_2S against other reducing gases. The high sensing performance of the structure was attributed to its nanoscale size, morphology and the disparity in the sensing mechanism between the H_2S and other reducing gases. We suggest that the work reported here including the simplicity of device fabrication is a significant step toward the application of ZnO nanomaterials in chemical gas sensing systems for the real-time detection of H_2S.

Keywords: ZnO; nanomaterial; H_2S; chemical sensor; gas sensor

1. Introduction

Hydrogen sulfide (H_2S) is a colorless, highly flammable and toxic gas [1]. It is produced due to industrial activities including petroleum refineries, natural gas plants, paper milling, sewage treatment plants and tanneries [2–5]. H_2S remains in the atmosphere from 1–42 days, depending on the season [6]. Its presence causes eye irritation, fatigue, headache, poor memory, dizziness, olfactory paralysis and respiratory distress. An increase in the concentration of H_2S up to 700 ppm causes human death [7]. Consequently, the monitoring of ambient H_2S levels, particularly in areas at hazardous waste sites, is needed. The information obtained can be used in combination with the known body burdens of H_2S to evaluate the potential risk of adverse health effects in the population. H_2S can also be released from meat, seafood, egg and milk products during their cooking and storage, and its production increases with the rise in temperature [8,9]. Thus, the detection of H_2S can be useful for the identification of food quality. The ingestion of food and water with high sulfur content increases urinary thiosulfate concentrations [10]. Moreover, blood sulfide levels were proposed as a biomarker [11]. Therefore, the development of small-size and portable H_2S gas sensors is in high demand to provide environmental and human health safety.

Metal oxides are very attractive materials for the fabrication of chemical sensors due to their ability to interact with different gaseous compounds [8,12–14]. In this aspect, the preparation of nanoscale oxide materials seems to be more efficient to improve their functional performance and opens new perspectives for their application in chemical gas sensors [15–19]. Low-dimensional metal oxide nanostructures with different shapes have been used to develop high-performance gas sensing systems [20–26]. To date, the most-studied material for chemical sensing applications is SnO_2 [27,28]. Other types of metal oxide nanostructures have been used as alternative materials to SnO_2 [25,29–31]. In recent years, much attention has been devoted to ZnO owing to its high electron mobility and thermal stability [16,32,33]. However, achieving a high response and selectivity of ZnO towards H_2S

is still a challenge. To enhance the gas sensing performance of ZnO it was functionalized with noble metal nanoparticles [34–36]. The noble metals improve the interaction of gaseous molecules with the sensing layer due to their catalytic activity [37–39]. Nevertheless, this is an expensive method and can increase the self-cost of the final device. In addition, the metal nanoparticles can lose their catalytic activity at relatively high operating temperatures due to the coagulation of particles on the support or can be poisoned by sulfur-containing chemical compounds [40,41]. Recently, the sensing properties of membrane-coated ZnO materials have been investigated. The obtained results have shown that it is an effective strategy to improve the materials selectivity [42,43]. To enhance the interaction between the gas molecules and sensing material, doped ZnO structures have been studied as well [15,16]. Some dopant materials decreased the optimal operating temperature of ZnO towards H_2S [44,45]. However, the operation of metal oxide-based sensors below 200 °C can be affected by water molecules, which worsen the material's recovery abilities [18]. The surface morphology and the structure of semiconductor materials have crucial effects on their sensing properties since the gas sensing process relies on the adsorption/desorption reactions of gas molecules on the surface of a material [46–52]. The synthesis of metal oxide nanostructures, varying their morphologies, improves their response towards specific gases [15]. In this regard, the synthesis of nanoscale oxide materials with special morphologies is conducted for the enhancement of their ability to interact with the target gas [15–17]. The fabrication of hierarchical nanostructures composed of aggregates of nanoparticles, which can act as reactive sites providing high surface area for the adsorption of gases, seems to be an effective strategy for the aforementioned purposes [30,53,54].

In this work, we present the synthesis and study of the gas sensing properties of ZnO nanomaterial for the detection of H_2S. We analyzed the gas sensing mechanism of the structure towards H_2S and investigated the selectivity against other reducing gases. We demonstrated that the morphology of the prepared ZnO is suitable to improve the absorption/desorption processes of oxygen and H_2S on the material, which affects the surface electronic structure of ZnO, enhancing its sensing response to H_2S. The operating temperature of the material and its interaction mechanism with the H_2S have a crucial effect on the response and selectivity of the sensing device. The results obtained show that the ZnO nanostructure exhibits an excellent sensing performance for potential applications in H_2S gas sensors.

2. Materials and Methods

ZnO nanomaterial was prepared based on our previously reported method with a few modifications, namely the anodization time and the applied potential [55]. First, metallic zinc films were deposited on 2 mm × 2 mm × 0.75 mm alumina substrates by means of radio-frequency (13.56 MHz) magnetron sputtering. The sputtering target was metallic zinc (purity 99.99%, 101.6 mm diameter, 6 mm thick, CAS number: 7440-66-6, Materion Advanced Chemicals Inc., Milwaukee, USA). The sputtering power and the time were 75 W and 35 min, respectively. To improve the adhesion of metallic films, the temperature of the alumina substrates was kept at 300 °C during the sputtering process. To perform the crystalline analysis of the materials, metallic zinc films were deposited on silicon substrates using the aforementioned sputtering regimes. Then, the metallic films were electrochemically anodized in a Teflon cell using a two-electrode system. The electrolyte solution was 2 M oxalic acid dihydrate ($C_2H_2O_4{\cdot}2H_2O$, ACS reagent, ≥99.5%, CAS number: 6153-56-6, Sigma-Aldrich, Inc., Steimhem, Germany) containing ethanol. A platinum foil was used as the cathode and the applied voltage during the anodization procedure was 20 V. The anodic oxidation procedure was performed at room temperature (RT) for 20 min. The anodized material was zinc oxalate dihydrate ($ZnC_2O_4{\cdot}2H_2O$). As-prepared materials were transformed to crystalline ZnO nanostructures by thermal decomposition process under a 50 vol% O_2/50 vol% Ar atmosphere at 500 °C for 8 h. To perform the gas sensing measurements, platinum electrodes with interdigital geometry were deposited onto the surface of obtained structures by means of radio-frequency magnetron sputtering. To carry out the sensing tests at different temperatures, a platinum heater was deposited on the backside of the substrates.

The crystal structure of the prepared material was studied with the X-ray diffraction spectroscopy (XRD) technique, using an Empyrean diffractometer (PANalytical, Almelo, The Netherlands) mounting a Cu-LFF (λ = 1.5406 Å) tube operated at 40 kV and 40 mA. The morphologies of the materials were examined by means of a LEO 1525 scanning electron microscope (SEM) equipped with a field emission gun (Carl Zeiss SMT AG, Oberkochen, Germany).

The gas sensing properties of the material were studied by a flow-through technique in a computer-controlled thermostatic test chamber. The detailed description of the experimental setup for the gas sensing measurements has been reported [56]. The carrier gas was humid synthetic air with a flow rate of 0.2 l/min and a relative humidity of 40%. Before the purging of analyte gas to the test chamber, the samples were stabilized for 10 h at each operating temperature. The conductance of samples was monitored by means of the volt-amperometric technique and the applied voltage was 1 V. The response (S) of structures was calculated according to the typical convention for the n-type semiconductor material: $S = \frac{(G_f - G_0)}{G_0} = \frac{\Delta G}{G_0}$, where G_0 is the sample conductance in air and G_f is the sample conductance in the presence of analyte gas [16,57].

3. Results and Discussions

3.1. Structural and Morphological Characterization

Figure 1a reports the XRD spectrum of the nanomaterial obtained on a silicon substrate. As can be seen, the as-prepared structure transformed to crystalline ZnO after the thermal treatment procedure at 500 °C. All the strong diffraction peaks in the spectrum were indexed to hexagonal wurtzite ZnO with lattice constants of a = 0.325 nm and c = 0.520 nm (JCPDS files no. 36-1451). The relative strength of the observed diffraction peaks perfectly matches with the hexagonal phase (JCPDS files no. 36-1451) [58,59]. Figure 1b shows the SEM images of the obtained ZnO nanomaterial with different resolutions. The morphological analyses indicate that the prepared materials have a nanosized structure, which consists of nanoparticles connected to each other and forming chains with lengths of a few microns. The average thickness of nanoparticles is 30 nm. Furthermore, the nanostructuration of metal oxide materials is an important issue, which determines their chemical sensing properties [16,46]. The synthesized ZnO material fully covered the surface of alumina substrates. Energy-dispersive X-ray (EDX) analyses were performed on different areas of the structure. The obtained EDX results confirmed the presence of Zn and O elements in the material with the Zn:O atomic ratio of 1:1 (Table 1).

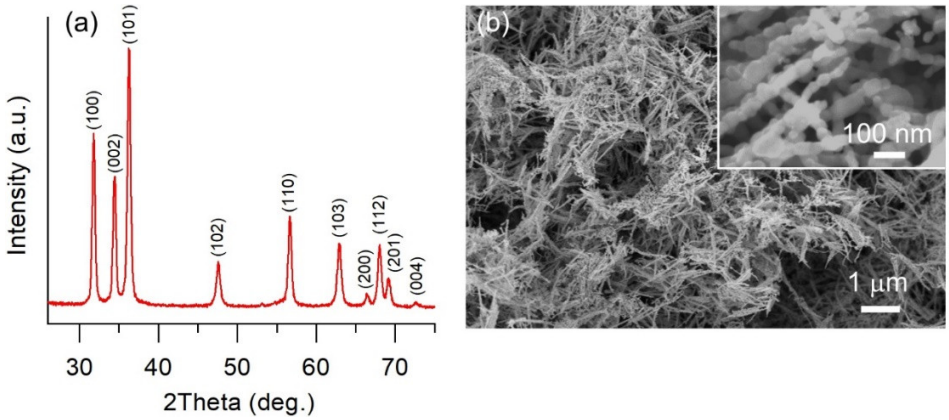

Figure 1. (**a**) X-ray diffraction (XRD) pattern of the ZnO nanomaterial obtained on a silicon substrate, (**b**) SEM images of the ZnO nanomaterial with different magnifications.

Table 1. Table of the quantitative analysis of the ZnO nanomaterial obtained by Energy-dispersive X-ray (EDX).

Element	Atomic % (±7%)
Zn	48

O 52

3.2. Gas Sensing Properties

In order to determine the optimal operating temperature of the obtained ZnO nanomaterials towards H_2S, we measured their gas sensing response at the operating temperatures of 200, 300, 400 and 500 °C. Figure 2a reports the relationship between the measured sensing response of the ZnO and its operating temperature. The response of structures increased with the temperature until 400 °C and decreased at 500 °C. The gas sensing mechanism of chemiresistive-type sensors is driven by reactions of the gaseous compounds with chemi- and physisorbed surface oxygen species [18,60,61]. Furthermore, the charge carriers have insufficient energy to overcome the barrier height energy at low working temperatures of the structure [13]. The sensing response of the oxide material at relatively low operating temperatures is mainly dominated by the physical adsorption process, where the gas molecules are adsorbed on the structure surface due to the van der Waals forces. The chemisorption process of H_2S is improved with the increase in the operating temperature of ZnO [18,62,63]. Thus, the reaction of the H_2S molecules with the ionosorbed oxygen species on the surface of ZnO was improved due to the increase of the sensor operating temperature, leading to an enhanced gas sensing response of the material. The reduced response at 500 °C can be attributed to the faster desorption rate of H_2S on the surface of the ZnO structure at high temperatures [62,63]. Consequently, the optimal operating temperature of the prepared ZnO nanomaterial towards H_2S is 400 °C. The sensitive performance of the ZnO was further investigated by exposing the structure to different concentrations of H_2S at its optimal operating temperature. The response amplitude of the ZnO sensor increased with the H_2S concentration (Figure 2b). The sensor showed responses of about 1, 1400, 6300 and 7400 towards 5, 10, 20 and 30 ppm of H_2S. The obtained response values show that the prepared ZnO nanomaterial has an excellent response towards relatively low concentrations of H_2S.

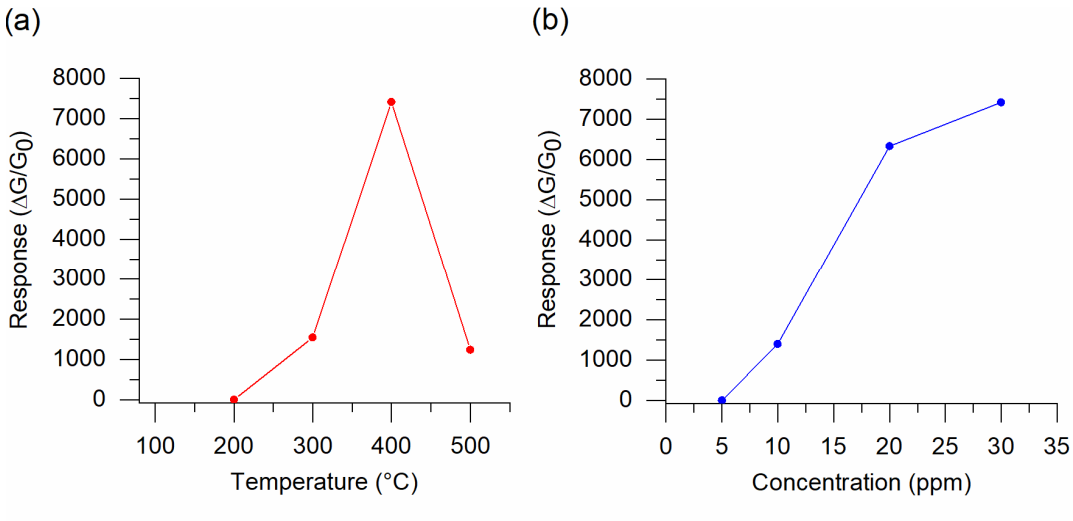

Figure 2. (**a**) Gas sensing response versus operating temperature dependence of the ZnO nanomaterial towards 30 ppm of H_2S. (**b**) Gas sensing response variation of the ZnO nanomaterial depending on the concentration of H_2S (5, 10, 20 and 30 ppm) at 400 °C.

Figure 3 presents the dynamical response of the ZnO structure towards 5, 10, 20 and 30 ppm of H_2S at 400 °C. It can be clearly seen that the conductance of the material increased rapidly when H_2S was introduced to the test chamber. After the H_2S flow was switched off, the conductance returned to the baseline, which confirms the reversible electrical response of the prepared ZnO nanomaterial towards H_2S. The conductance increase of the structure upon interaction with a reducing gas is typical behavior for an n-type oxide material such as ZnO [64]. The aforementioned conduction change mechanism of the ZnO can be explained as follows: The oxygen was ionosorbed on the surface of the ZnO (typically as O^-) under exposure to air at 400 °C (Equation (1)). Thus, an electron-

depleted layer was formed on the surface of the material, increasing the surface potential [18,61]. When the sensing structure was exposed to the H_2S, the depletion layer was narrowed, followed by a decrease in the surface potential caused by the chemical reactions between the ionosorbed oxygen and H_2S molecules (Equation (2)) [65]. Consequently, the electrical conductance of material was increased. In addition, the H_2S molecules can adsorb in metastable configurations on the surface of ZnO at relatively high operating temperatures [66]. Therefore, the sulfuration and desulfuration reversible reactions can occur between the H_2S and ZnO (Equations (3) and (4)). These reactions occur simultaneously without creating the stable intermediate product of ZnS. However, the sulfuration reaction influences the capability of oxygen to extract electrons from ZnO. That is to say, the ZnO nanostructure plays a role similar to the catalyst [67,68].

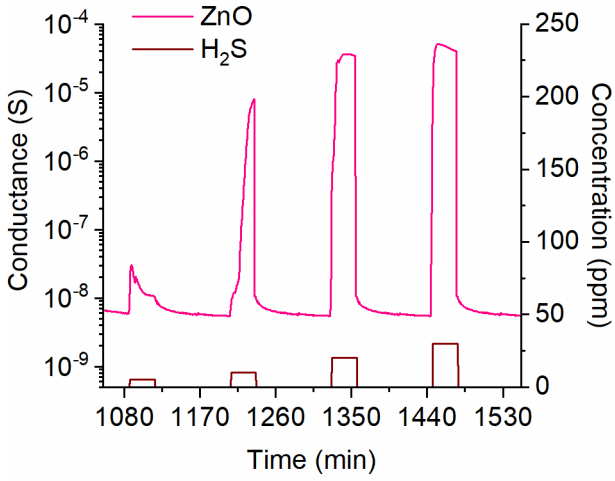

Figure 3. Dynamical response of the ZnO nanomaterial towards 5, 10, 20 and 30 ppm of H_2S at 400 °C.

$$O_2 + 2e^- \rightarrow 2O^- \quad (1)$$

$$H_2S + 3O^- \rightarrow H_2O + SO_2 + 3e^- \quad (2)$$

$$H_2S + ZnO \rightarrow H_2O + ZnS \quad (3)$$

$$2ZnS + 3O_2 \rightarrow 2ZnO + 2SO_2 \quad (4)$$

The sensing properties of the prepared ZnO nanomaterial towards H_2S were compared with that of previously reported H_2S gas sensors based on ZnO (Table 2). The obtained ZnO material showed a significant improvement in gas sensing response compared with the other structures at their optimal operating temperatures. Moreover, the obtained samples have an advantage in their sensing performance compared to some of the doped and mixed ZnO structures at their optimal working conditions. The higher gas sensing response of the obtained material towards H_2S was attributed to its morphology, which induced effective diffusion as well as providing a larger effective surface area due to the form and porosity of the structure. In this case, the chains were composed of nanoparticles connected to each other, forming a very high surface area and thereby enhancing the response of the ZnO material.

Table 2. Comparison of H_2S gas sensing properties of the prepared ZnO nanomaterial with the previously reported H_2S gas sensors based on ZnO. G_0 is the sample conductance in air and G is the sample conductance in the presence of H_2S. R_0 is the sample resistance in air, R is the sample resistance in the presence of H_2S.

Composition and Morphology	Operating Temperature (°C)	Gas Concentration (ppm)	Response	Ref.
ZnO nanorods	500	50	$\Delta G/G_0$, 35	[69]
ZnO dendrites	30	100	R_0/R, 17,3	[70]
ZnO nanoparticles	300	20	$\Delta R/R_0$, 0.8	[71]

ZnO nanorods	50	100	G/G_0, 61.7	[72]
ZnO nanowires	150	20	R/R_0, ~0.9	[68]
ZnO comb-like	RT	4	$\Delta R/R_g$, 0.8	[73]
Al–ZnO	200	150	R_0/R, 2.05	[45]
Cu–ZnO nanograins	250	10	$\Delta R/R_0$, ~0.9	[74]
Au–ZnO nanorods	RT	6	G_g/G_0, 1270	[34]
Carbon–ZnO nanofibers	250	30	R/R_0, 77.75	[75]
Pd–SnO_2–ZnO	RT	20	R_0/R, 0.064	[44]
ZnO	400	20	$\Delta G/G_0$, 6300	This work

The selectivity of the fabricated ZnO sensors was studied towards 20 ppm of ammonia (NH_3), dimethylamine (DMA) and acetone (C_3H_6O) at the optimal operating temperature of 400 °C (Figure 4). The responses of the material towards NH_3 and C_3H_6O were 2 and 0.4, respectively. The structure was not sensitive towards DMA at 400 °C. Instead, the response towards H_2S was about 6300. The results obtained indicate that the prepared ZnO nanomaterial has a high selectivity towards H_2S against other interfering gases. This significant difference in the structure sensing response towards H_2S and other interfering gases can be related to the sulfuration and desulfuration reversible reactions on the surface of the material. Since the aforementioned reactions were not involved in the sensing mechanism of the ZnO towards interfering gases, the material showed a weaker response to them. Thus, the disparity in the sensing mechanism between H_2S and other reducing gases could be the reason for the better sensing performance of ZnO towards H_2S.

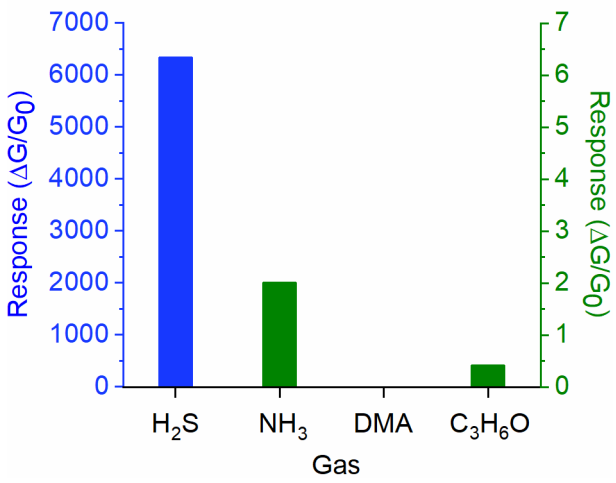

Figure 4. Response of the obtained ZnO nanomaterial towards 20 ppm of H_2S, NH_3, dimethylamine (DMA) and C_3H_6O at 400 °C. The response towards H_2S was very high compared to the other gases. To visualize the response values towards all the gases the response of the structure towards H_2S is shown in blue (left axis), and the response towards NH_3, DMA and C_3H_6O is shown in green (right axis).

4. Conclusions

In summary, we have reported the synthesis and investigations of chemical sensing properties of ZnO nanomaterial for the detection of H_2S. The material was fabricated by the electrochemical anodization method and thermal decomposition procedure. The structure consists of nanoparticles connected to each other, forming chains with the length of a few microns. The nanoparticles (diameter ~30 nm) and the chain-like morphology of the structure increased the surface area for the interaction between the material and H_2S gas. The ZnO nanomaterial exhibited n-type semiconducting behavior based on the electrical measurements. Furthermore, the fabricated sensors showed high sensing response and selectivity towards H_2S gas. The excellent sensing performance of the prepared ZnO nanomaterial was attributed to its morphology, the operating temperature and the disparity in the sensing mechanism between H_2S and other reducing gases. The obtained results demonstrate the potential suitability of the application of ZnO in gas sensing devices for the detection of H_2S.

Author Contributions: The authors contributed equally to this work.

Funding: This research received no external funding.

Conflicts of Interest: The authors declare no conflict of interest.

References

1. Morsali, M.; Rezaei, M. Assessment of H_2S emission hazards into tunnels: The nosoud tunnel case study from Iran. *Environ. Earth Sci.* **2017**, *76*, 227.
2. Nassar, I.M.; Noor El-Din, M.R.; Morsi, R.E.; El-Azeim, A.A.; Hashem, A.I. Eco friendly nanocomposite materials to scavenge hazard gas H_2S through fixed-bed reactor in petroleum application. *Renew. Sustain. Energy Rev.* **2016**, *65*, 101–112.
3. Catalan, L.; Liang, V.; Johnson, A.; Jia, C.; O'Connor, B.; Walton, C. Emissions of reduced sulphur compounds from the surface of primary and secondary wastewater clarifiers at a kraft mill. *Environ. Monit. Assess.* **2008**, *156*, 37.
4. Bandosz, T.J.; Le, Q. Evaluation of surface properties of exhausted carbons used as H_2S adsorbents in sewage treatment plants. *Carbon* **1998**, *36*, 39–44.
5. Zahn, J.A.; DiSpirito, A.A.; Do, Y.S.; Brooks, B.E.; Cooper, E.E.; Hatfield, J.L. Correlation of human olfactory responses to airborne concentrations of malodorous volatile organic compounds emitted from swine effluent. *J. Environ. Qual.* **2001**, *30*, 624–634.
6. Bottenheim, J.W.; Strausz, O.P. Gas-phase chemistry of clean air at 55.Degree. N latitude. *Environ. Sci. Technol.* **1980**, *14*, 709–718.
7. Chou, C.H.; Selene, J. *Hydrogen Sulfide: Human Health Aspects*; World Health Organization & International Programme on Chemical Safety: Geneva, Switzerland, 2003.
8. Galstyan, V.; Bhandari, M.; Sberveglieri, V.; Sberveglieri, G.; Comini, E. Metal oxide nanostructures in food applications: Quality control and packaging. *Chemosensors* **2018**, *6*, 16.
9. Roach, K.A.; Tobler, M.; Winemiller, K.O. Hydrogen sulfide, bacteria, and fish: A unique, subterranean food chain. *Ecology* **2011**, *92*, 2056–2062.
10. Milby, T.H.; Baselt, R.C. Hydrogen sulfide poisoning: Clarification of some controversial issues. *Am. J. Ind. Med.* **1999**, *35*, 192–195.
11. Jappinen, P.; Vilkka, V.; Marttila, O.; Haahtela, T. Exposure to hydrogen-sulfide and respiratory-function. *Br. J. Ind. Med.* **1990**, *47*, 824–828.
12. Comini, E.; Faglia, G.; Sberveglieri, G. *Solid State Gas. Sensing Preface*; Springer: New York, NY, USA, 2009; pp. 47–99.
13. Yamazoe, N.; Shimanoe, K. Theory of power laws for semiconductor gas sensors. *Sens. Actuators B Chem.* **2008**, *128*, 566–573.
14. Catto, A.C.; da Silva, L.F.; Ribeiro, C.; Bernardini, S.; Aguir, K.; Longo, E.; Mastelaro, V.R. An easy method of preparing ozone gas sensors based on ZnO nanorods. *RSC Adv.* **2015**, *5*, 19528–19533.
15. Spencer, M.J.S. Gas sensing applications of 1d-nanostructured zinc oxide: Insights from density functional theory calculations. *Prog. Mater. Sci.* **2012**, *57*, 437–486.
16. Galstyan, V.; Comini, E.; Ponzoni, A.; Sberveglieri, V.; Sberveglieri, G. ZnO quasi-1d nanostructures: Synthesis, modeling, and properties for applications in conductometric chemical sensors. *Chemosensors* **2016**, *4*, 6.
17. Galstyan, V.; Comini, E.; Faglia, G.; Sberveglieri, G. TiO_2 nanotubes: Recent advances in synthesis and gas sensing properties. *Sensors* **2013**, *13*, 14813–14838.
18. Galstyan, V. Porous TiO_2-based gas sensors for cyber chemical systems to provide security and medical diagnosis. *Sensors* **2017**, *17*, 2947.
19. Semenova, D.; Gernaey, K.V.; Silina, Y.E. Exploring the potential of electroless and electroplated noble metal–semiconductor hybrids within bio- and environmental sensing. *Analyst* **2018**, *143*, 5646–5669.
20. Li, J.; Fu, T.; Chen, Y.; Guan, B.; Zhuo, M.; Yang, T.; Xu, Z.; Li, Q.; Zhang, M. Highly sensitive humidity sensors based on Sb-doped $ZnSnO_3$ nanoparticles with very small sizes. *CrystEngComm* **2014**, *16*, 2977–2983.
21. Huang, H.-W.; Liu, J.; He, G.; Peng, Y.; Wu, M.; Zheng, W.-H.; Chen, L.-H.; Li, Y.; Su, B.-L. Tunable macro-mesoporous ZnO nanostructures for highly sensitive ethanol and acetone gas sensors. *RSC Adv.* **2015**, *5*, 101910–101916.

22. Ha, N.H.; Thinh, D.D.; Huong, N.T.; Phuong, N.H.; Thach, P.D.; Hong, H.S. Fast response of carbon monoxide gas sensors using a highly porous network of ZnO nanoparticles decorated on 3d reduced graphene oxide. *Appl. Surf. Sci.* **2018**, *434*, 1048–1054.
23. Zhang, M.; Ning, T.; Sun, P.; Yan, Y.; Zhang, D.; Li, Z. Effect of Al_2O_3-SiO_2 substrate on gas-sensing properties of TiO_2 based lambda sensor at high temperature. *Ceram. Int.***2018**, *44*, 3000-3004.
24. Sun, L.; Fang, W.; Yang, Y.; Yu, H.; Wang, T.; Dong, X.; Liu, G.; Wang, J.; Yu, W.; Shi, K. Highly active and porous single-crystal In_2O_3 nanosheet for NO_x gas sensor with excellent response at room temperature. *RSC Adv.* **2017**, *7*, 33419–33425.
25. Galstyan, V.; Comini, E.; Baratto, C.; Ponzoni, A.; Ferroni, M.; Poli, N.; Bontempi, E.; Brisotto, M.; Faglia, G.; Sberveglieri, G. Large surface area biphase titania for chemical sensing. *Sens. Actuators B Chem.* **2015**, *209*, 1091–1096.
26. Hyun, S.K.; Sun, G.-J.; Lee, J.K.; Lee, C.; In Lee, W.; Kim, H.W. Ethanol gas sensing using a networked PbO-decorated SnO_2 nanowires. *Thin Solid Films* **2017**, *637*, 21–26.
27. Das, S.; Jayaraman, V. SnO_2: A comprehensive review on structures and gas sensors. *Prog. Mater. Sci.* **2014**, *66*, 112–255.
28. Zhao, Y.; Zhang, W.; Yang, B.; Liu, J.; Chen, X.; Wang, X.; Yang, C. Gas-sensing enhancement methods for hydrothermal synthesized SnO_2-based sensors. *Nanotechnology* **2017**, *28*, 452002.
29. Poongodi, S.; Kumar, P.S.; Mangalaraj, D.; Ponpandian, N.; Meena, P.; Masuda, Y.; Lee, C. Electrodeposition of WO_3 nanostructured thin films for electrochromic and H_2S gas sensor applications. *J. Alloys Compd.* **2017**, *719*, 71–81.
30. Chava, R.K.; Cho, H.-Y.; Yoon, J.-M.; Yu, Y.-T. Fabrication of aggregated In_2O_3 nanospheres for highly sensitive acetaldehyde gas sensors. *J. Alloys Compd.* **2019**, *772*, 834–842.
31. Choi, S.; Bonyani, M.; Sun, G.-J.; Lee, J.K.; Hyun, S.K.; Lee, C. Cr_2O_3 nanoparticle-functionalized WO_3 nanorods for ethanol gas sensors. *Appl. Surf. Sci.* **2018**, *432*, 241–249.
32. Li, F.M.; Hsieh, G.-W.; Dalal, S.; Newton, M.C.; Stott, J.E.; Hiralal, P.; Nathan, A.; Warburton, P.A.; Unalan, H.E.; Beecher, P.; et al. Zinc oxide nanostructures and high electron mobility nanocomposite thin film transistors. *IEEE Trans. Electron. Devices* **2008**, *55*, 3001–3011.
33. Vakulov, Z.E.; Zamburg, E.G.; Khakhulin, D.A.; Ageev, O.A. Thermal stability of ZnO thin films fabricated by pulsed laser deposition. *Mater. Sci. Semicond. Process.* **2017**, *66*, 21–25.
34. Hosseini, Z.S.; Mortezaali, A.; Iraji zad, A.; Fardindoost, S. Sensitive and selective room temperature H_2S gas sensor based on Au sensitized vertical ZnO nanorods with flower-like structures. *J. Alloys Compd.* **2015**, *628*, 222–229.
35. Kim, H.; Pak, Y.; Jeong, Y.; Kim, W.; Kim, J.; Jung, G.Y. Amorphous Pd-assisted H_2 detection of ZnO nanorod gas sensor with enhanced sensitivity and stability. *Sens. Actuators B Chem.* **2018**, *262*, 460–468.
36. Wongrat, E.; Chanlek, N.; Chueaiarrom, C.; Thupthimchun, W.; Samransuksamer, B.; Choopun, S. Acetone gas sensors based on ZnO nanostructures decorated with Pt and Nb. *Ceram. Int.* **2017**, *43*, S557–S566.
37. Liu, J.; Wang, W.; Shen, T.; Zhao, Z.; Feng, H.; Cui, F. One-step synthesis of noble metal/oxide nanocomposites with tunable size of noble metal particles and their size-dependent catalytic activity. *RSC Adv.* **2014**, *4*, 30624–30629.
38. Yang, M.-Q.; Pan, X.; Zhang, N.; Xu, Y.-J. A facile one-step way to anchor noble metal (Au, Ag, Pd) nanoparticles on a reduced graphene oxide mat with catalytic activity for selective reduction of nitroaromatic compounds. *CrystEngComm* **2013**, *15*, 6819–6828.
39. Tian, H.; He, J.; Liu, L.; Wang, D. Effects of textural parameters and noble metal loading on the catalytic activity of cryptomelane-type manganese oxides for formaldehyde oxidation. *Ceram. Int.* **2013**, *39*, 315–321.
40. Subramanian, V.; Wolf, E.E.; Kamat, P.V. Influence of metal/metal ion concentration on the photocatalytic activity of TiO_2−Au composite nanoparticles. *Langmuir* **2003**, *19*, 469–474.
41. Arnal, P.M.; Comotti, M.; Schüth, F. High-temperature-stable catalysts by hollow sphere encapsulation. *Angew. Chem. Int. Ed.* **2006**, *45*, 8224–8227.
42. Weber, M.; Kim, J.-H.; Lee, J.-H.; Kim, J.-Y.; Iatsunskyi, I.; Coy, E.; Drobek, M.; Julbe, A.; Bechelany, M.; Kim, S.S. High-performance nanowire hydrogen sensors by exploiting the synergistic effect of Pd nanoparticles and metal–organic framework membranes. *ACS Appl. Mater. Interfaces* **2018**, *10*, 34765–34773.
43. Drobek, M.; Kim, J.-H.; Bechelany, M.; Vallicari, C.; Leroy, E.; Julbe, A.; Kim, S.S. Design and fabrication of highly selective H_2 sensors based on SIM-1 nanomembrane-coated ZnO nanowires. *Sens. Actuators B Chem.* **2018**, *264*, 410–418.

44. Kim, H.; Jin, C.; Park, S.; Lee, C. Enhanced H_2S gas sensing properties of multiple-networked Pd-doped SnO_2-core/ZnO-shell nanorod sensors. *Mater. Res. Bull.* **2012**, *47*, 2708–2712.
45. Kolhe, P.S.; Shinde, A.B.; Kulkarni, S.G.; Maiti, N.; Koinkar, P.M.; Sonawane, K.M. Gas sensing performance of al doped ZnO thin film for H_2S detection. *J. Alloys Compd.* **2018**, *748*, 6–11.
46. Yamazoe, N.; Shimanoe, K. Roles of shape and size of component crystals in semiconductor gas sensors. *J. Electrochem. Soc.* **2008**, *155*, J85–J92.
47. Brunet, E.; Maier, T.; Mutinati, G.C.; Steinhauer, S.; Koeck, A.; Gspan, C.; Grogger, W. Comparison of the gas sensing performance of SnO_2 thin film and SnO_2 nanowire sensors. *Sens. Actuators B Chem.* **2012**, *165*, 110–118.
48. Wei, S.H.; Wang, S.M.; Zhang, Y.; Zhou, M.H. Different morphologies of ZnO and their ethanol sensing property. *Sens. Actuators B Chem.* **2014**, *192*, 480–487.
49. Zhang, J.; Song, P.; Li, Z.; Zhang, S.; Yang, Z.; Wang, Q. Enhanced trimethylamine sensing performance of single-crystal MoO_3 nanobelts decorated with Au nanoparticles. *J. Alloys Compd.* **2016**, *685*, 1024–1033.
50. Lim, Y.T.; Son, J.Y.; Rhee, J.S. Vertical ZnO nanorod array as an effective hydrogen gas sensor. *Ceram. Int.* **2013**, *39*, 887–890.
51. Barillaro, G.; Bruschi, P.; Lazzerini, G.M.; Strambini, L.M. Validation of the compatibility between a porous silicon-based gas sensor technology and standard microelectronic process. *IEEE Sens. J.* **2010**, *10*, 893–899.
52. Galstyan, V.E.; Martirosyan, K.S.; Aroutiounian, V.M.; Arakelyan, V.M.; Arakelyan, A.H.; Soukiassian, P.G. Investigations of hydrogen sensors made of porous silicon. *Thin Solid Films* **2008**, *517*, 239–241.
53. Suematsu, K.; Shin, Y.; Hua, Z.; Yoshida, K.; Yuasa, M.; Kida, T.; Shimanoe, K. Nanoparticle cluster gas sensor: Controlled clustering of SnO_2 nanoparticles for highly sensitive toluene detection. *ACS Appl. Mater. Interfaces* **2014**, *6*, 5319–5326.
54. Li, Y.; Song, Z.; Li, Y.; Chen, S.; Li, S.; Li, Y.; Wang, H.; Wang, Z. Hierarchical hollow MoS_2 microspheres as materials for conductometric NO_2 gas sensors. *Sens. Actuators B Chem.* **2019**, *282*, 259–267.
55. Galstyan, V.; Comini, E.; Baratto, C.; Ponzoni, A.; Bontempi, E.; Brisotto, M.; Faglia, G.; Sberveglieri, G. Synthesis of self-assembled chain-like ZnO nanostructures on stiff and flexible substrates. *Crystengcomm* **2013**, *15*, 2881–2887.
56. Barreca, B.; Gasparotto, A.; Maccato, C.; Maragno, C.; Tondello, E.; Comini, E.; Sberveglieri, G. Columnar CeO_2 nanostructures for sensor application. *Nanotechnology* **2007**, *18*, 125502.
57. Sysoev, V.V.; Goschnick, J.; Schneider, T.; Strelcov, E.; Kolmakov, A. A gradient microarray electronic nose based on percolating SnO_2 nanowire sensing elements. *Nano Lett.* **2007**, *7*, 3182–3188.
58. Kundu, S. A facile route for the formation of shape-selective ZnO nanoarchitectures with superior photo-catalytic activity. *Colloids Surf. A Physicochem. Eng. Asp.* **2014**, *446*, 199–212.
59. Galeazzi, R.; González-Panzo, I.J.; Díaz-Becerril, T.; Morales, C.; Rosendo, E.; Silva, R.; Romano-Trujillo, R.; Coyopol, A.; Nieto-Caballero, F.G.; Treviño-Yarce, L. Physicochemical conditions for ZnO films deposited by microwave chemical bath deposition. *RSC Adv.* **2018**, *8*, 8662–8670.
60. Schroeder, S.; Gottfried, J.M. *Temperature-Programmed Desorption (TPD) Thermal Desorption Spectroscopy (TDS)*; Advanced Physical Chemistry Laboratory, FU: Berlin, Germany, 2002; pp. 1–22.
61. Galstyan, V.; Comini, E.; Kholmanov, I.; Ponzoni, A.; Sberveglieri, V.; Poli, N.; Faglia, G.; Sberveglieri, G. A composite structure based on reduced graphene oxide and metal oxide nanomaterials for chemical sensors. *Beilstein J. Nanotechnol.* **2016**, *7*, 1421–1427.
62. Shaw, D.J. 5—the solid–gas interface. In *Introduction to Colloid and Surface Chemistry*, 4th ed.; Shaw, D.J., Ed.; Butterworth-Heinemann: Oxford, UK, 1992; pp. 115–150.
63. Shaw, D.J. 7—charged interfaces. In *Introduction to Colloid and Surface Chemistry*, 4th ed.; Shaw, D.J., Ed.; Butterworth-Heinemann: Oxford, UK, 1992; pp. 174–209.
64. Morrison, S.R. The adsorbate-free surface. In *The Chemical Physics of Surfaces*; Morrison, S.R., Ed.; Springer: Boston, MA, USA, 1977; pp. 99–149.
65. Wetchakun, K.; Samerjai, T.; Tamaekong, N.; Liewhiran, C.; Siriwong, C.; Kruefu, V.; Wisitsoraat, A.; Tuantranont, A.; Phanichphant, S. Semiconducting metal oxides as sensors for environmentally hazardous gases. *Sens. Actuators B Chem.* **2011**, *160*, 580–591.
66. Goclon, J.; Meyer, B. The interaction of H_2S with the ZnO (100) surface. *Phys. Chem. Chem. Phys.* **2013**, *15*, 8373–8382.
67. Wang, D.; Chu, X.; Gong, M. Hydrothermal growth of ZnO nanoscrewdrivers and their gas sensing properties. *Nanotechnology* **2007**, *18*, 185601.

68. Huang, H.; Xu, P.; Zheng, D.; Chen, C.; Li, X. Sulfuration–desulfuration reaction sensing effect of intrinsic ZnO nanowires for high-performance H_2S detection. *J. Mater. Chem. A* **2015**, *3*, 6330–6339.
69. Kim, J.; Yong, K. Mechanism study of ZnO nanorod-bundle sensors for H_2S gas sensing. *J. Phys. Chem. C* **2011**, *115*, 7218–7224.
70. Zhang, N.; Yu, K.; Li, Q.; Zhu, Z.Q.; Wan, Q. Room-temperature high-sensitivity H_2S gas sensor based on dendritic ZnO nanostructures with macroscale in appearance. *J. Appl. Phys.* **2008**, *103*, 104305.
71. Mortezaali, A.; Moradi, R. The correlation between the substrate temperature and morphological ZnO nanostructures for H_2S gas sensors. *Sens. Actuators A Phys.* **2014**, *206*, 30–34.
72. Shinde, S.D.; Patil, G.E.; Kajale, D.D.; Gaikwad, V.B.; Jain, G.H. Synthesis of ZnO nanorods by spray pyrolysis for H_2S gas sensor. *J. Alloys Compd.* **2012**, *528*, 109–114.
73. Faisal, A.D. Synthesis of ZnO comb-like nanostructures for high sensitivity H_2S gas sensor fabrication at room temperature. *Bull. Mater. Sci.* **2017**, *40*, 1061–1068.
74. Girija, K.G.; Somasundaram, K.; Topkar, A.; Vatsa, R.K. Highly selective H_2S gas sensor based on Cu-doped ZnO nanocrystalline films deposited by RF magnetron sputtering of powder target. *J. Alloys Compd.* **2016**, *684*, 15–20.
75. Zhang, J.; Zhu, Z.; Chen, C.; Chen, Z.; Cai, M.; Qu, B.; Wang, T.; Zhang, M. ZnO-carbon nanofibers for stable, high response, and selective H_2S sensors. *Nanotechnology* **2018**, *29*, 275501.